Los Alamos NATIONAL LABORATORY EST.1943

LA-UR-21-26570 (Accepted Manuscript)

High-level fuel fabrication facility designs from discrete-event simulation

Bourque, Cade Michael
Clarno, Kevin T.
Leibowicz, Benjamin D.

Provided by the author(s) and the Los Alamos National Laboratory (2022-01-03).

To be published in: Annals of Nuclear Energy

DOI to publisher's version: 10.1016/j.anucene.2021.108893

Permalink to record: http://permalink.lanl.gov/object/view?what=info:lanl-repo/lareport/LA-UR-21-26570

Disclaimer:
Los Alamos National Laboratory, an affirmative action/equal opportunity employer, is operated by Triad National Security, LLC for the National Nuclear Security Administration of U.S. Department of Energy under contract 89233218CNA000001. By approving this article, the publisher recognizes that the U.S. Government retains nonexclusive, royalty-free license to publish or reproduce the published form of this contribution, or to allow others to do so, for U.S. Government purposes. Los Alamos National Laboratory requests that the publisher identify this article as work performed under the auspices of the U.S. Department of Energy. Los Alamos National Laboratory strongly supports academic freedom and a researcher's right to publish; as an institution, however, the Laboratory does not endorse the viewpoint of a publication or guarantee its technical correctness.

Research Library

High-Level Fuel Fabrication Facility Designs from Discrete-Event Simulation

Cade M. Bourque*, Kevin T. Clarno†, Benjamin D. Leibowicz†

*Los Alamos National Laboratory, PT-3, P.O. Box 1663, Los Alamos, New Mexico 87544, cbourque@lanl.gov

†The University of Texas at Austin, 204 E. Dean Keeton St., Austin, TX 78712, clarno@utexas.edu, bleibowicz@utexas.edu

Corresponding Author: Cade M. Bourque

Abstract

Like other industrial processes, the production of metallic nuclear fuels (MNF) requires that fabrication facilities be able to reliably meet production demands, operate efficiently, and adhere to federal and local safety regulations. In turn, the set of design variables employed by such a facility, such as operations policies, infrastructure and machinery purchased, and the type and number of staff hired, directly impact a facility's ability to satisfy these goals. Therefore, facility designers must carefully determine which set of design variable values optimally satisfies these constraints. In this paper, we explore how values for these high-level design variables, namely hiring requirements, can be determined in the context of nuclear fuel manufacturing through the coupling of physics-based and discrete-event simulation technologies. Using the Versatile Test Reactor (VTR) program as a case study, we demonstrate how SCALE and MCNP nuclear physics model outputs can be integrated into ExtendSim discrete-event simulation (DES) models of the fuel fabrication process to determine the optimal number of staff hired to ensure fuel production goals are met, operations comply with effective dose limit regulations, and overall project costs are reduced.

Keywords

Discrete-Event Simulation, Optimization

Highlights

- k_{eff} limits will not be a binding design constraint, as criticality never exceeds 0.566 in any alloy-geometry configuration
- Dose rates vary between 0.0272 and 554.0 mrem/h and are dependent on both alloy selection and which step in the fabrication process a worker is executing
- To adequately staff fuel production, anywhere from 28 to 63 individuals will need to be hired, depending on which set of design constraints are active
- Under baseline design constraints, the MNF fabrication facility is estimated to incur a total project cost of $777.7M
- This total can be reduced by as much as $43.3M if the production confidence constraint is relaxed to P(throughput - $\sigma \geq 40$ assemblies/yr) = 0.95
- Utilization of U-20Pu-10Zr alloy containing 6,000 ppm ^{241}Am is unlikely, due to excessive hiring requirements to comply with effective dose limits

1. Introduction

To support production of metallic nuclear fuel (MNF) at a nuclear facility, operational policies and facility designs must be established to ensure fuel fabrication processes satisfy production demands while also adhering to local and federal safety regulations. Design constraints, such as fuel alloy selection and dose rate and criticality limitations, and the reliability with which production demands are met, dictate operations and facility design choices, and the value of these design variables, encompassing everything from minimum staffing requirements to identifying the scale of infrastructure and machinery needed, must be carefully chosen to ensure MNF fabrication facilities are optimized to minimize project costs and maximize efficiency across its projected 10 yr lifetime.

This paper seeks to outline a method by which physics simulation software, SCALE [1] and MCNP6.2 [2], and discrete-event simulation (DES) software, ExtendSim Pro 10 [3], can be coupled to assist in the determination of the optimal value of these design variables. To demonstrate this, we use the development of the Versatile Test Reactor (VTR) program as a test case. This program, developed by the United States Department of Energy (DoE) in 2017 with the goal of restoring advanced material and fuel testing to the US, may require the creation of a new MNF fabrication facility to support "in-house" production of VTR fuel. The physics and discrete-event models developed for this study reflect the fuels and pin-casting processes that could be employed to fuel the VTR and are subject to the baseline design constraints (summarized in Table 1) which are representative of design constraints the MNF fabrication facility supplying the VTR mission may face [4][5].

Design Constraint	Value
Alloy Selection	UPuAmZr-0.03
Scheduling	5 days/week, 8 hours/day
Criticality Limit	$k_{eff} \leq 0.9$
Effective Dose Limit	$E \leq 2{,}000$ mrem/year
Throughput Confidence	P(throughput - $2\sigma \geq 40$ assemblies/yr) = 0.95
Glove Box Consolidation	Disallowed

Table 1: Baseline DES design constraints.

2. Methodology

2.1. Generation of Radiological Data

The first step in deriving feasible design variable values is to properly characterize the radiological profile of the nuclear fuel being fabricated. To calculate the effective dose rates generated by the UPuZr fuel in various geometries and isotopic compositions, one must first establish the intrinsic source terms associated with the unirradiated fuel. This is accomplished by modeling the decay of the fuel with respect to its isotopic composition and corresponding atomic density in ORIGEN.

A unique decay model is constructed and run for each of the representative fuel compositions listed in Table 2. Since the potential fuel feedstock has a wide range of compositions and the age of the ^{241}Pu defines the Am concentration via beta decay, three representative compositions were identified to simulate:

- Weapons-grade Pu in a U-20Pu-10Zr fuel with a low (0.03%) Am content (UPuAmZr-0.03)
- Weapons-grade Pu in a U-20Pu-10Zr fuel with a high (0.6%) Am content (UPuAmZr-0.6)
- U-10Zr (UZr)

In each ORIGEN simulation, the fuel alloy decays for a year in an unirradiated environment, with neutron and photon particle intensity metrics being recorded at the times listed in Table 3. Because there will be a time-delay from production of the fuel feedstock billets and fabrication of the fuel rods, these time periods account for a range of radiation decay and daughter product buildup after production. Additionally, by modeling the alloys over this timeframe, an intensity-time relationship can be derived for an alloy's neutron and photon radiation source terms while the fuel is being fabricated.

	Alloy		
Nuclide	UPuAmZr-0.6	UPuAmZr-0.03	UZr
^{234}U	0.0002	0.0002	0.0003
^{235}U	0.0350	0.0350	0.0450
^{236}U	0.0002	0.0002	0.0002
^{238}U	0.6646	0.6646	0.8545
^{239}Pu	0.1800	0.1857	0.0000
^{240}Pu	0.0140	0.0140	0.0000
Zr	0.1000	0.1000	0.1000
^{241}Am	0.0060	0.0003	0.0000

Table 2: Fuel isotopic composition. All values represent initial isotopic composition for each alloy in wt%. [1][6]

Sample	Sample Time (d)
1	0
2	1
3	5
4	7
5	14
6	30
7	180
8	365

Table 3: Sample times in SCALE simulations.

Running each alloy through ORIGEN creates the source term neutron and gamma radiation profiles. The neutrons and photons in each model are binned according to energy, and each energy bin is assigned an intensity value representing the fraction of all particles contained within the energy bin. This creates discrete energy distributions for the neutron and photons for each alloy composition, which are later used in MCNP6.2 to define the source. Throughout the course of the fabrication process, the fuel alloy will adopt four basic geometric forms:

1. Lumped Cube (LC): a cube of the raw alloy (Figure A.1)
2. Cast Pin Array (CPA): 61 soda lime glass encased pins arranged in a hexagonal array with a pitch of 1 cm (Figure A.2)
3. Finished Pin Array (FPA): 61finished pins (i.e. cylindrical fuel pins encased in type 304 stainless steel cladding and metallic sodium) arranged in a hexagonal array with a 1 cm pitch (Figure A.3)
4. Fuel Assembly (FA): 434 finished pins arranged into two 217-unit hexagonal arrays (each with a pitch of 1 cm) stacked vertically on top of each other (Figures A.3-A.5)

These forms are not literal recreations of the actual fuel form-factors one would expect to observe in practice; rather, these are representative forms that approximate the geometries expected to assume during the fuel assembly fabrication process.

In addition to the four basic geometric configurations illustrated above, five additional geometric arrangements are modeled to explore how dose rates and criticality respond for when consolidated glove box operations are permitted by the design constraints (i.e. multiple steps of the fabrication process are permitted to occur in a single glove box). These are represented via:

1. One lumped cube and one cast pin array per glove box (LC - CPA)
2. Two cast pin arrays per glove box (2 CPA)
3. One finished pin array and one cast pin array per glove box (CPA - FPA)
4. Two fuel assemblies per glove box (2 FA)
5. Three fuel assemblies per glove box (3 FA)

Allowing multiple processes to occur in a single glove box reduces the overall number of glove boxes needed for fuel fabrication activities, dually lowering infrastructure investments (and therefore total project costs) and reducing the overall footprint of said fuel fabrication facility design. However, it also has the potential increase worker dose and approach criticality limits.

For each alloy-geometry configuration, three MCNP6.2 input decks are run to generate three sets of data: neutron effective dose rate, photon effective dose rate, and reactivity estimates. Across each of these test scenarios, the geometry of the working environment is largely the same; a MIRD-ORNL-Male voxel phantom [7] stands at the center of a 7.42 x 2.49 x 4.38 m (width, depth, and height, respectively) [4] room whose ceiling and floor are modeled as 10.16 cm thick concrete. These dimensions approximate the environment at the Fuel Manufacturing Facility at INL (a potential location for MNF fabrication activities) and represent a glove box laterally surrounded by a 0.46 m buffer. All exterior planes (including those above and below the concrete ceiling and floor) are modeled as reflective boundaries to simulate an infinite array of glove boxes, all of which contain identical quantities of nuclear material. The MIRD phantom, standing 15 cm away from the glove box, is modeled with arms reaching into an argon-filled glove box via two glove holes equipped with 1.5 cm-thick butyl gloves to simulate a worker handling the nuclear fuel.

The glove box has dimensions of 78 x 38 x 84 in and is raised 37.25 in off the ground, with steel and leaded glass sides with dimensions listed in Table 4 [4][8]. Lastly, while the geometry of the fuel varies depending on its configuration (Figures A.1-A.5), the fuel is always positioned in the center of the glove box, resting on the base plate of the glove box.

Side	Material	Thickness (cm)
Front	Leaded Glass	1.270
Back	Leaded Glass	1.270
Top	Type 304 SS	0.476
Bottom	Type 304 SS	1.905
Left	Type 304 SS	0.476
Right	Type 304 SS	0.476

Table 4: Glove box component dimensions.

MCNP6.2 testing occurs in three phases: criticality simulations, neutron effective dose rate simulations, and photon effective dose rate simulations. The parameters governing these tests (described below) are identical across all alloy-geometry models, barring source particle intensities and energy distributions. These source particle and energy parameters are set to reflect the values derived from SCALE testing for each given alloy-geometry configuration.

For criticality simulations, 200 total cycles, with 170 active cycles, of 50,000 source histories each cycle are simulated to estimate the reactivity of the system. These cycle and history counts were chosen to ensure all criticality estimates embodied standard deviations less than 0.001. Regardless of geometric configuration, the MCNP6.2 source definition treats all fuel-containing cells as neutron sources and is equally likely to both sample any fuel-containing cell out of all total fuel cells and sample any point within each fuel containing cell as a source point. Criticality findings will help determine whether a spatial layout and working mass of nuclear material at a given process adhere to criticality safety guidelines. Meanwhile, dose rate findings inform the staffing requirements needed to conduct said process.

For both neutron and photon effective dose rate tests, the energy distribution of source particles is specified on the SDEF card to match the energy spectrum of 180-day old fuel alloy from the ORIGEN simulation. This alloy age is chosen due to the neutron and photon profiles of the fuel alloys having reached relative equilibrium, which represents a reasonable maximum source-term. For the dose simulations, like the criticality source, the source definition treats all fuel-containing cells as neutron or gamma sources and is equally likely to both sample any fuel containing cell out of all total fuel cells and sample any point within each fuel containing cell as a source point.

F4 tallies are used to determine the average cell flux across an energy spectrum for different cells of the voxel phantom. The number of particle histories run for dose rate calculations are 20 and 500 million for neutron and photon dose rate tests, respectively. These values are sufficiently large to keep overall tally errors below 5%. Errors

above 5% are generally considered unreliable, invalidating all but the highest-level findings derived with such data [2]. Additionally, low-error (i.e. approximately 1% error) findings were required in this stage to ensure the effects of dose rate and criticality uncertainty did not noticeably affect results gathered in the DES portion of this study, which itself contains elements that include stochastic uncertainties.

Following the MCNP6.2 simulations, the collected F4 tally data for both neutron and photon tests are grouped according to alloy-geometry configuration, and the combined neutron-photon effective dose rate is calculated using Eq. 1, in which i, j, and k define all particle types, energies, and materials, respectively, and ϕ, $\Re$, and N represent the particle flux, response function [9], and particle source strength, respectively.

$$\left(\sum_{i}^{n,ph}\left(\sum_{j}^{energy\ (MeV)}\left(\sum_{k}^{material\ type}\phi_{i,j,k}\frac{1}{cm^2}\right)\cdot\Re_j(E)\frac{mrem\cdot cm^2}{particle}\right)\right)\cdot N_i\frac{particles}{s}=\dot{E}\frac{mrem}{s} \qquad \text{Eq. 1}$$

For each energy bin extracted from the MCNP6.2 output, the flux is first multiplied by the appropriate dose coefficient and then every dose-weighted flux is summed together to produce a dose burden per-source particle.

In multiplying this value by the source particle intensities determined with SCALE, a particle type-dependent effective dose rate in units of mrem/hour can be derived for a given alloy-geometry configuration. To calculate the final effective dose rate, the neutron and photon dose rate findings are simply summed together.

The total dose burden of a given task in the fabrication process dictates the minimum number of full-time workers needed to maintain year-long operation of said task without exposing any individual worker beyond their annual dose limit, which would be organizationally defined and comply with the NRC limits for radiation workers (5 rem/yr). For this study, a 2 rem/yr limit will serve as the effective dose limit. This reduced effective dose limit is representative of annual dose limits that institutions, such as the DOE laboratories, integrate into their ALARA ("as low as reasonably achievable") practices [5]. While other mechanisms such as installing shielding exist for reducing dose and, in turn, personnel requirements, this paper does not explore this possibility; rather, this study focuses solely on how operations decisions can be leveraged to lower costs and dose burdens.

2.2. DES Model Creation and Optimization

With criticality and dose rate values determined for every alloy-geometry configuration, the process of estimating employee dose can begin. The DES models employed by this study are structured around the injection-casting pin production manufacturing process once employed by Argonne National Laboratory to produce MNF in support of the EBR-II [10]. This design, illustrated in Figure 1, both describes a MNF casting process which may be suitable for VTR fuel production and characterizes the basic material input demands, processing times, and material flow information required to construct a working DES model which accurately simulates MNF fabrication activities. From this framework, this rudimentary model is optimized to minimize costs following a procedure outlined by Bourque et al (2021) [11]. In following this procedure, the system is restructured to ensure the facility both reliably and efficiently meets production demands. Upon creating this initial model which conforms to the constraints listed in Table 1, the entire process is restarted to produce 11 other DES models to produce a total of 12 MNF fabrication facility designs which conform to the twelve sets of design constraints listed in Table 5.

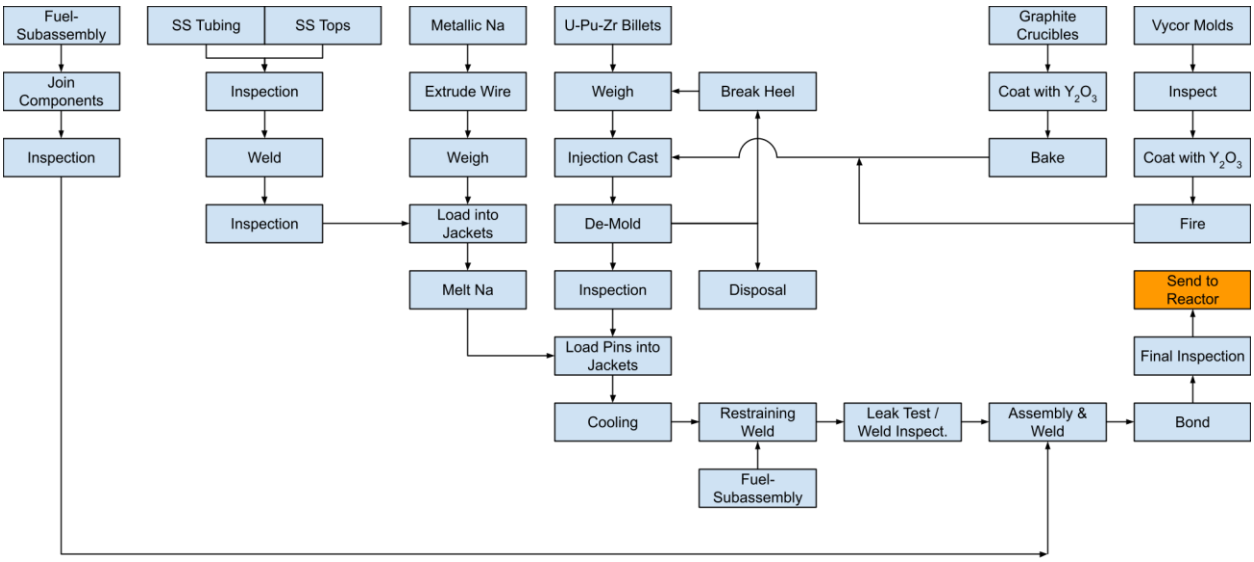

Figure 1: High-level material flowchart of the metallic nuclear fuel fabrication process [10].

	Scenario #	Alloy	Hrs/Day	Dose Limit	Confidence	Consolid.?
Alloy Selection	1	UZr	8	2 rem/y	$\mu - 2\sigma \geq 40$	No
	2	UPuAmZr-0.03	8	2 rem/y	$\mu - 2\sigma \geq 40$	No
	3	UPuAmZr-0.6	8	2 rem/y	$\mu - 2\sigma \geq 40$	No
4-10 Schedule	4	UZr	10	2 rem/y	$\mu - 2\sigma \geq 40$	No
	5	UPuAmZr-0.03	10	2 rem/y	$\mu - 2\sigma \geq 40$	No
	6	UPuAmZr-0.6	10	2 rem/y	$\mu - 2\sigma \geq 40$	No
Strict Dose Limit	7	UPuAmZr-0.03	8	0.5 rem/y	$\mu - 2\sigma \geq 40$	No
	8	UPuAmZr-0.03	10	0.5 rem/y	$\mu - 2\sigma \geq 40$	No
Lowered Confidence	9	UPuAmZr-0.03	8	2 rem/y	$\mu - \sigma \geq 40$	No
	10	UPuAmZr-0.03	10	2 rem/y	$\mu - \sigma \geq 40$	No
Condensed Operation	11	UPuAmZr-0.03	8	2 rem/y	$\mu - 2\sigma \geq 40$	Yes
	12	UZr	8	2 rem/y	$\mu - 2\sigma \geq 40$	Yes

Table 5: Testing scenarios and their corresponding constraints.

2.3. Physics Simulation-DES Integration

The next step in this process is integrating the radiological profiles of the various alloy-geometry fuel configurations into the DES model. Dose rate data generated during ORIGEN and MCNP6.2 testing are imported into ExtendSim Pro 10 models of the optimized injection casting MNF fabrication process via "constant" blocks [10][3]. In the ExtendSim environment, processes which require workers to handle radioactive materials are represented as "activity" blocks, which are able to record the total simulated time said process was actively being performed (i.e., a worker was directly manipulating fuel). In these models, the recorded uptime value for a given process is then multiplied by a "constant" block whose value is equal to the corresponding dose rate in units of mrem/h (Tables B.1 & B.2). The product is defined as the process-specific dose burden imposed by one year of MNF production, E_{task}^{j}, where *j* designates the classification of the task (e.g., whether the task was executed by welders or general laborers). Overall, the sum of all E_{task}^{j} is the total annual class-specific dose burden, E_{tot}^{j}. While in practice many more work classifications are expected to exist, from the set of activities included in our DES model, only welding tasks require workers to perform a specialized skill. This ability is what distinguishes "welders" from "general labor", and is the grounds on which the decision to bar welders from performing general labor tasks, and vice versa, is founded.

Upon the completion of a simulation, these class-specific totals are divided by the minimum number of employees belonging to each class necessary to meet production MNF assembly goals, n_j, to calculate the average dose received by the individual employee, $\bar{E}^j$. If this quantity is below the limit described in the design constraint, L, we are able to validate that models satisfies all design constraints and we can conclude that the currently-implemented set of operation policies and floorplans adhere to safety requirements. However, if this value exceeds the dose limit constraint, redundancy hires must be made so that new workers can replace those who reach their dose limits. The scale of this redundancy hiring is embodied by the hiring safety multiplier, *HSM*, and is calculated for both general labor and welder using Eq. 2.

$$HSM_j = \left\lceil \frac{E_{tot}^j / L}{n_j} \right\rceil \quad \text{Eq. 2}$$

2.4. Cost Analysis

The overall project cost of the VTR program is a metric used in comparing the relative feasibility of the possible VTR configurations outlined in Table 5, and is calculated by summing the total costs incurred across four types of expenses: input material costs, employee wages, overhead (a term whose value is defined as five times the cost incurred by employee wages), and infrastructure investments [12]. The representative per-unit and hourly costs employed in this study are outlined in Tables C.1-C.4. Our estimate of the VTR program's cost is calculated with Eq. 3, which, using the terms defined in Table 6, sums the initial infrastructure purchases costs with annual expenses on materials purchasing, employee compensation (assuming workers perform 1,600 hours of work per year), and other recurring costs. Assuming a ten-year lifespan for the VTR (the period during which the VTR's impact on industrial and scientific operational and economics will be evaluated) [6], a 2.27% inflation rate is incorporated into the value of these latter, on-going expenses to account for the expected effects of economic inflation.

$$C = \sum_{i=0}^{9} \left[\sum_j M_j m_j f_j + (1 + OM) \cdot \sum_l (W_l w_l \cdot 1{,}600) \right] \cdot 1.0227^i + \sum_k R_k r_k \quad \textit{Eq. 3}$$

Variable		Meaning
Exogenous	M_j	Material type, j
	m_j	Per-unit cost of material, j
	w_l	Wage of worker of class l
	OM	Overhead multiplier
	R_k	Units of infrastructure of type k
	r_k	Per-unit cost of infrastructure of type k
Endogenous	f_j	Frequency of purchase of material, j
	W_l	Number of workers in class, l

Table 6: Variable definitions for VTR lifetime cost equation, Eq. 3.

3. Results

3.1. Dose Rate and Criticality Results

When the methodology described above is applied to the VTR test cases in described, we discover the following; first, MCNP6.2 criticality estimations indicate that criticality limits will not be a limiting factor in the design of facility layouts. As detailed in Tables 7 & 8, below, average k_{eff} values across all alloy-geometry configurations range between 0.07466 and 0.36401. With a 99% confidence interval, these values are extended to $0.07452 \leq k_{eff} \leq 0.36425$. Assuming facilities enforce a strict subcriticality limit of 0.9, even the most active, densely arranged alloy-geometry configuration (i.e. UPuAmZr-0.6 in lumped cube form) will still embody a safety factor of over 2.4.

Configuration	$k_{eff} \pm \sigma$ UZr	UPuAmZr-0.03	UPuAmZr-0.6
LC	0.2370 ± 0.0001	0.3640 ± 0.0001	0.3602 ± 0.0001
CPA	0.0747 ± 0.0001	0.1089 ± 0.0001	0.1082 ± 0.0001
FPA	0.1610 ± 0.0001	0.2234 ± 0.0001	0.2211 ± 0.0001
FA	0.1611 ± 0.0001	0.2246 ± 0.0001	0.2219 ± 0.0001

Table 7: Criticality values for basic alloy-geometry configurations.

Configuration	$k_{eff} \pm \sigma$ UZr	UPuAmZr-0.03
LC – CPA	0.2370 ± 0.0001	0.3638 ± 0.0001
2 CPA	0.0834 ± 0.0001	0.1176 ± 0.0001
CPA - FPA	0.1555 ± 0.0001	0.2185 ± 0.0001
2 FPA	0.1932 ± 0.0001	0.2564 ± 0.0001
3 FA	0.2292 ± 0.0001	0.2928 ± 0.0001

Table 8: Criticality values for consolidated glove box configurations.

An additional, accident-case scenario, in which a lumped cube and cast-pin array of UPuAmZr-0.03 (the most critical configuration) was placed in a glove box filled with room-temperature water, was modeled and run in MCNP6.2 to study its effect on criticality. The water, acting as a moderator and reflector, did result in an increase in k_{eff}, raising criticality from 0.36401 to 0.56559. However, this value is still far below the assumed 0.9 criticality limit. These findings suggest that, at any stage in the fuel fabrication process, either the current material mass limits can be substantially increased or the spacing between glove boxes can be substantially decreased without fear of exceeding subcriticality limits. However, the extent to which this is valid is not yet known and would require further study.

Estimated effective dose rates are dominated by the photon-based ionizing radiation and are highly dependent on the isotopic composition and geometric configuration of the fuel. This volatility results in calculated effective dose rates with values that span three orders of magnitude, ranging from a minimum of $0.0273 \pm 1.49 \times 10^{-4}$ mrem/h to a maximum of 55.4 ± 0.073 mrem/h.

As illustrated in Figures 2 & 3, the smallest of these effective dose rates are exhibited by fuels crafted from UZr alloys. As the fuel alloy is changed to include higher concentrations of transuranic content, the effective dose rate progressively grows. By replacing UZr with UPuAmZr-0.03 or UPuAmZr-0.6 alloys, the effective dose rate increases by an average of 3,226% and 30,696%, respectively. A distinct trend can be observed in terms of the fuel's geometry as well; across all alloys, dose rates are minimized when in the lumped cube configuration and are maximized when in fuel assembly configuration.

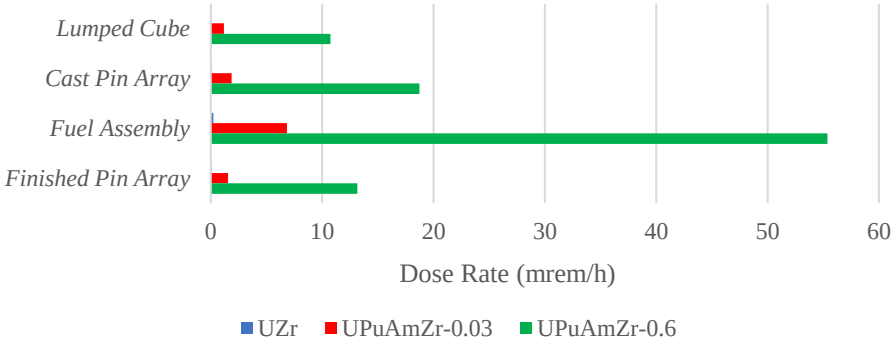

Figure 2: Coupled bar graph of effective dose rates for all basic alloy-geometry configurations.

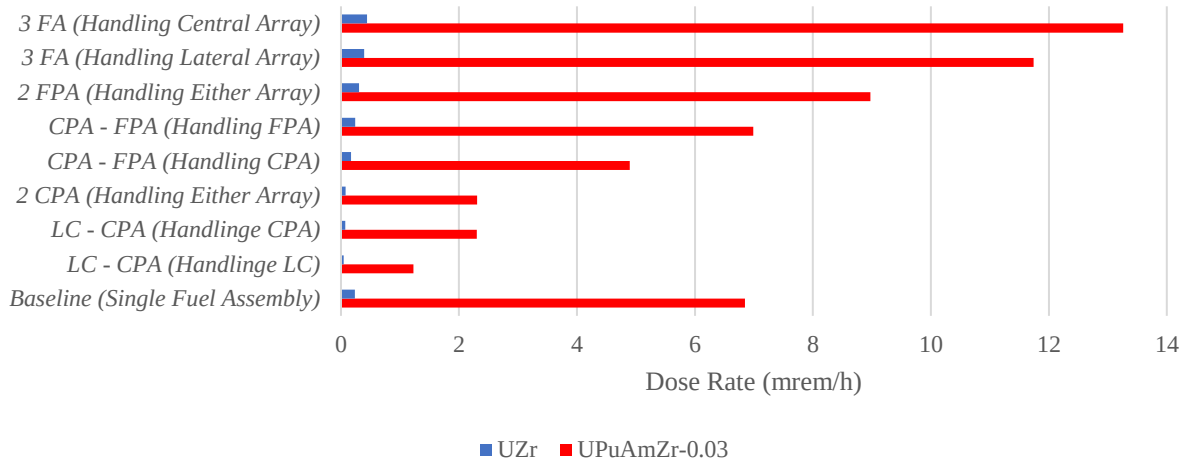

Figure 3: Coupled bar graph of effective dose rates for all consolidated alloy-geometry configurations.

Dose rates for fuels in consolidated glove box arrangements span values from $0.0481 \pm 3.17 \times 10^{-4}$ to $0.441 \pm 2.74 \times 10^{-3}$ for scenarios in which UZr fuel is employed and 1.23 ± 0.106 to 13.3 ± 0.189 for scenarios in which UPuAmZr-0.03 fuel is employed. These findings suggest that dose rate does not respond to consolidation in a purely additive manner; the total estimated dose rates from a given configuration are less than the sum of the dose rates from the individual fuel geometries in the system.

This paper does not explore test cases in which UPuAmZr-0.6 fuel is handled in a consolidated glove box environment, as the dose rates exhibited by UPuAmZr-0.6 fuels in basic geometric configurations were already alarmingly high, and would require untenable levels of redundancy hires to be made for said configurations to be viable. This effect would only be exaggerated in consolidated glove box arrangements, and thus was not explored as a possible test scenario.

3.2. DES Results

To generate cost, production, and dose rate estimations for evaluation, each of the 12 DES models is run 100 times. This quantity was chosen as it would provide ample data points to adequately characterize the distribution of outcomes for each model while also being fast enough to run as to not incur excessive computational expenses (nominally, 2 hours per 100 runs). As detailed in Figure 5, lifetime costs for the VTR program are highly sensitive to changes in design constraint values, exhibiting average lifetime program expenses ranging from $717.7M to $827.4M. The highest of these lifetime costs occur when design constraints stipulate that the UPuAmZr-0.6 alloy is to be employed as the working fuel; in both Scenarios 3 & 6, program costs rise in excess of $824M, a 6.40% increase over the baseline configuration (Scenario 2). Similarly, Scenarios 7 & 8, configurations in which dose limits are reduced to 0.5 rem/y also incur increased program costs, reaching totals of $795.2M and $791.2M, respectively.

Conversely, scenarios in which scheduling, infrastructure demands, and production reliability standards are adjusted and/or relaxed yield savings relative to our baseline configuration. These effects, detailed in Table 9, range from marginal to significant; adopting a 4-10 work schedule (a consolidated work schedule in which workers work four ten-hour shifts per week instead of the typical five eight-hour shifts) returns savings of just $4.0M. Meanwhile, lowering production throughput confidence and allowing for consolidated glove box operations reduce total equivalent cost of the VTR by $43.3 and $40.0M, respectively.

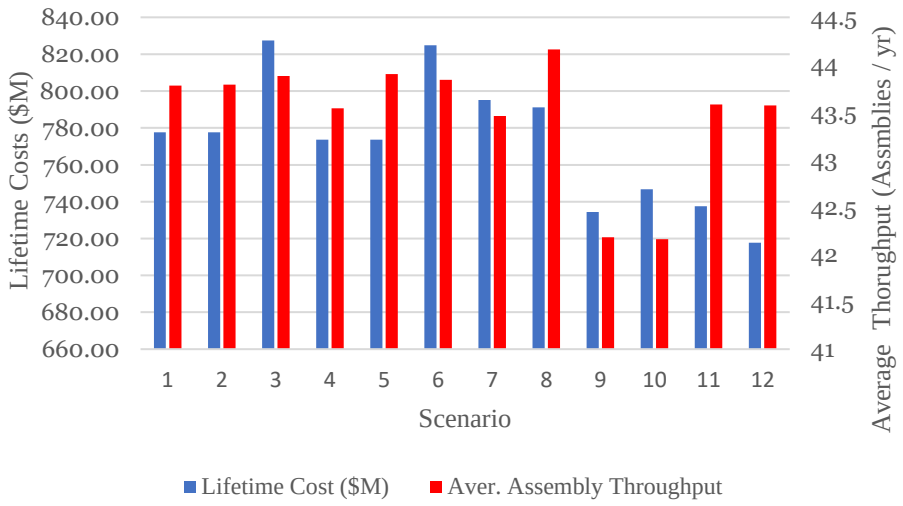

Figure 4: Total equivalent costs of the VTR fuel fabrication facility and throughput metrics by scenario.

	Lifetime Cost ($M)			
Design Constraint	Minimum	Maximum	Change (-/+)	% Change (-/+)
Alloy	777.7	827.4	0 / 49.8	0 / 6.40
Schedule	773.7	777.7	-4.0 / 0	-0.51 / 0
Dose Limit	777.7	795.2	0 / 17.6	0 / 2.26
Production Confidence	734.3	777.7	-43.3 / 0	-5.57 / 0
Consolidation	737.6	777.7	-40.0 / 0	-5.15 / 0

Table 9: Project lifetime cost changes due to changes in single design constraints relative to Scenario 2.

Unlike project cost, fuel assembly production metrics respond subtlety as changes in design constraints are applied. As illustrated in Figure 4 and detailed in Table 10, average assembly production throughput assumes values between 42.16 and 44.16 assemblies/yr, a 4.63% difference across all scenarios. In all cases, average throughput satisfies the 40 assemblies/yr constraint and average throughput values follow normal distributions. However, in order to satisfy the production target with 95% confidence, the MNF fabrication facility must overshoot their production goals by as much as 10.4%. This suggests that increased manufacturing reliability could be a mechanism for reducing cost, as limiting the number of excess assemblies produced would decrease material and employee costs. Conversely, this excess production may be necessary for reliability; in cases where the production line fails to meet the 40 assemblies/yr goal, having surplus assemblies on-hand may be a vital means of ensuring the VTR is not starved for fuel assemblies. Future studies will need to be conducted to determine which operational policy is preferable.

Scenario No.	Average Throughput, μ	Std. Dev., σ	Per-Assembly Cost ($K)
Scenario 1	43.78	1.33	1,805.6
Scenario 2	43.79	1.37	1,805.2
Scenario 3	43.88	1.40	1,914.9
Scenario 4	43.54	1.82	1,809.4
Scenario 5	43.90	1.59	1,794.6
Scenario 6	43.84	1.56	1,913.9
Scenario 7	43.46	1.65	1,859.3
Scenario 8	44.16	1.60	1,823.8
Scenario 9	42.18	1.29	1,771.4
Scenario 10	42.16	1.77	1,804.7
Scenario 11	43.58	1.49	1,708.6
Scenario 12	43.57	1.62	1,663.4

Table 10: Average annual fuel assembly throughput and standard deviation values for each scenario.

Figure 5 illustrates the average annual effective dose workers will receive when working under each of the 12 scenarios explored before redundancy hires are made to reduce individuals' dose rates below the 2,000 mrem/y limit. Across all configurations, annual effective dose rates for general labor assume values spanning three orders of magnitude, ranging from 32.68 to 13,238.31 mrem/yr. Similarly, the average dose rates to welders range from 43.29 to 23,755.70 mrem/y.

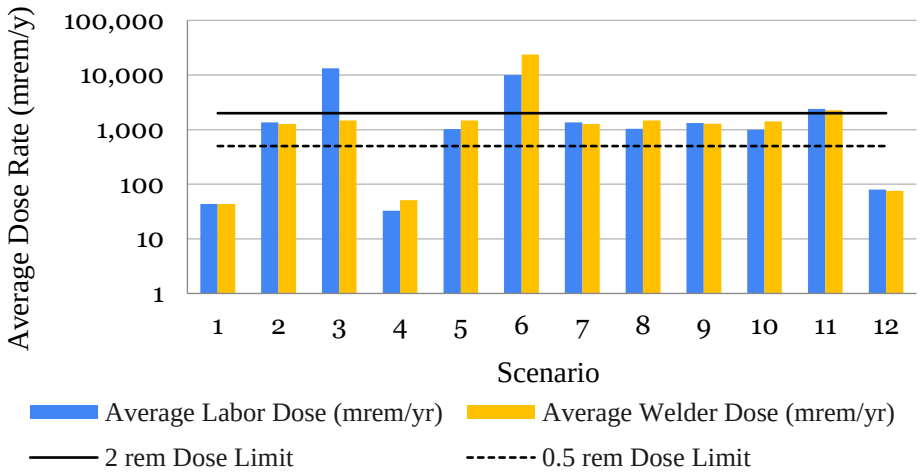

Figure 5: Average dose to personnel by job and scenario plotted on semi-log scale.

As expected, scenarios which employ UZr as the working fuel deliver effective annual dose rates that are approximately one and two orders of magnitude below their UPuAmZr-0.03 and UPuAmZr-0.6 counterparts, respectively; across all UZr-employing scenarios, annual effective dose rates remain 79.72 mrem/yr for both general labor and welders, meaning redundancy hiring will not be required if UZr fuels are utilized.

In contrast, the selection of UPuAmZr-0.03 only requires redundancy hiring in three scenarios: Scenarios 7, 8, and 11. In these circumstances where dose limits are lowered (i.e. Scenarios 7 & 8), annual dose rates range from 1,028 to 1,479 mrem/yr, requiring a tripling in staffing requirements. Likewise, in Scenario 11, where glove box operations are spatially consolidated, dose rates reach 2,401 mrem/y for general laborers and 2,253 mrem/yr for welders. This results in staffing requirements needing to be doubled in order to comply with the 2,000 mrem/yr limit. The number of workers required under each scenario is detailed in Table 11.

Scenario No.	No. of General Labor	No. of Welders	Total Personnel
1	17	11	28
2	17	11	28
3	41	21	62
4	17	11	28
5	17	11	28
6	42	21	63
7	25	15	40
8	25	15	40
9	17	11	28
10	16	11	27
11	21	13	34
12	17	11	28

Table 11: Minimum number of workers required by facility configuration.

Conclusions

Through coupling physics and discrete-event simulation technologies via the methodology described above, we were able to successfully derive satisfactorily optimal facility designs and operations policies for each of the 12 proposed VTR configurations. In examining the results generated by this study, we are dually able to approximate the optimal design of the MNF fabrication facility needed to support "in-house" fuel production for the VTR and extract key insights as to how changes to said facility's design variables drive overall project costs.

In order to produce a minimum of 40 fuel assemblies per year while maintaining a production confidence level exceeding 95%, and to prevent individual employees from exceeding their annual dose limit of 2 rem/yr, the following investments must be made:

Personnel / Infrastructure	Minimum Requirements
Welders	11
General Labor	17
Pin Casting Lanes	3
Jacket Production Lanes	4
Na-Bonding Lanes	3
Crucible & Vycor Production Lanes	2
Glove Boxes	16

Table 12: Baseline facility configuration personnel and infrastructure requirements.

With this configuration, the MNF fabrication facility produces an average of 43.79 fuel assemblies per year with a 95% confidence level. Additionally, general workers incur an average annual effective dose of 1,261 mrem, while their welder counterparts absorb a similar 1,358 mrem. Overall, in this configuration, the VTR incurs an equivalent monthly cost of $6.587M, leading to a project lifetime cost of $777.658M, assuming a 2.27% annual inflation rate.

However, if design constraints can be adjusted to lower total equivalent costs, one can reduce the lifetime total by $43.309M – a 5.57% decrease. As depicted in Table 9, allowing either the production confidence constraint (Scenarios 9 & 10) or consolidated glove box constraint (Scenarios 11 & 12) to be relaxed yields savings in the form of reduced material purchasing and/or reduced infrastructure needs. Shifting operations to a 4-10 schedule (Scenarios 4-6) could potentially result in modest savings, reducing lifetime costs by roughly $3.978M. However, this option would incur the consequence of needing to purchase extra infrastructure (i.e. an additional pin casting lane). Conversely, lowering dose limits to 0.5 rem/y strictly leads to significant increases in cost, adding as much as $ 17.5M to the lifetime project costs. These increased costs stem from the need to make redundancy hires in order to be dose limit-compliant.

Overall, in coupling physics simulation and DES technologies, one can effectively derive high-level insights into how one can craft a safe and cost-optimized MNF fabrication facility. As demonstrated by our results, a new MNF

fabrication facility should consider embracing and modifying historic facility designs and operational policies to reflect the configuration modeled in Scenarios 9, 11, or 12. In each of these cases, MNF production occurs under a 5-8 schedule in consolidated glove boxes. Additionally, workers would be limited to an annual effective dose of 2 rem/y and the facility will aim to meet minimum production goals with a minimum of 68.3% confidence. These configurations would require the following decisions to be made:

	Minimum Requirements		
Personnel / Infrastructure	Scenario 9	Scenario 11	Scenario 12
Welders	11	13	11
General Labor	17	21	17
Pin Casting Lanes	3	3	3
Jacket Production Lanes	4	4	4
Na-Bonding Lanes	3	3	3
Crucible & Vycor Production Lanes	2	2	2
Glove Boxes	16	9	9

Table 13: Facility configuration, personnel, and infrastructure requirements for Scenarios 9, 11, & 12.

While configuring a facility to resemble Scenario 9 would yield significant savings over its Scenario 2 counterpart, the reduced production confidence could potentially lead to situations in which the MNF fabrication facility cannot independently supply the VTR with enough fuel to remain operational. This could be detrimental to the success of the VTR program, so a careful risk analysis should be performed before this option is seriously considered.

Acknowledgements

The lead author would like to thank both the University of Texas at Austin and Los Alamos National Laboratory for sponsoring this project. This project was intended to develop and understanding of the neutronics and design processes for a fuel fabrication facility and in no way represents the design of the actual VTR fuel fabrication facility. More detailed discussion of the DES process is documented in [11]. The authors acknowledge the Texas Advanced Computing Center (TACC) at The University of Texas at Austin for providing HPC resources that have contributed to the research results reported within this paper. URL: http://www.tacc.utexas.edu.

LA-UR-21-26570

Funding

This research was funded by both the University of Texas at Austin and Los Alamos National Laboratory.

Appendix A: Geometric Forms

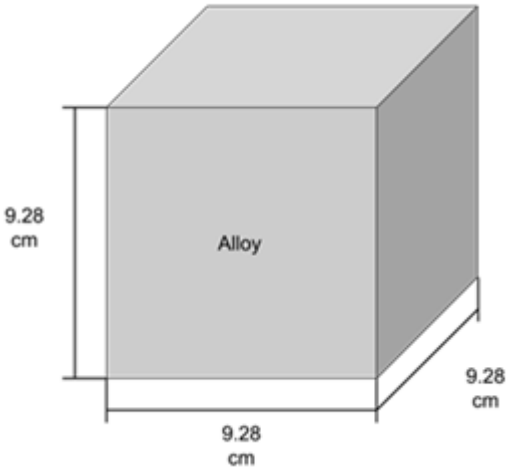

Figure A.1: Lumped cube geometric configuration.

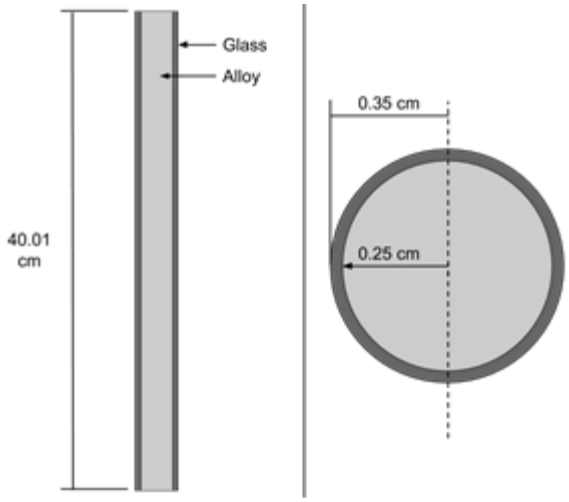

Figure A.2: Cast pin geometric configuration, viewed laterally (left) and from above (right). In MCNP6.2 models, 61 of these pins are arranged in a hexagonal array with a pitch of 1 cm.

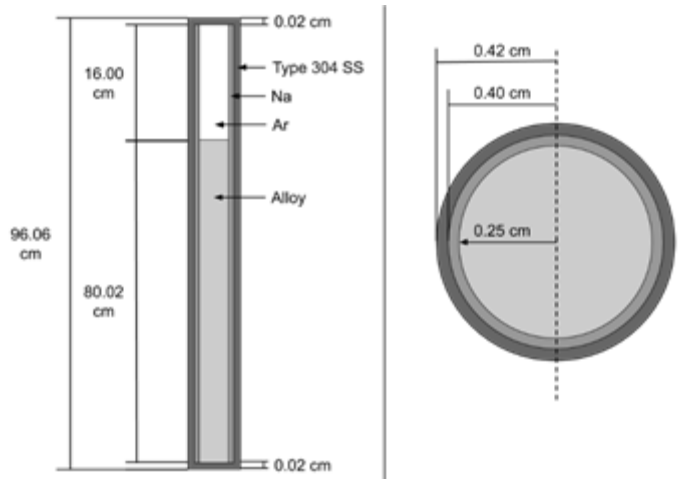

Figure A.3: Finished pin geometric configuration, viewed laterally (left) and from above (right). In MCNP6.2 models, 61 of these pins are arranged in a hexagonal array with a pitch of 1 cm.

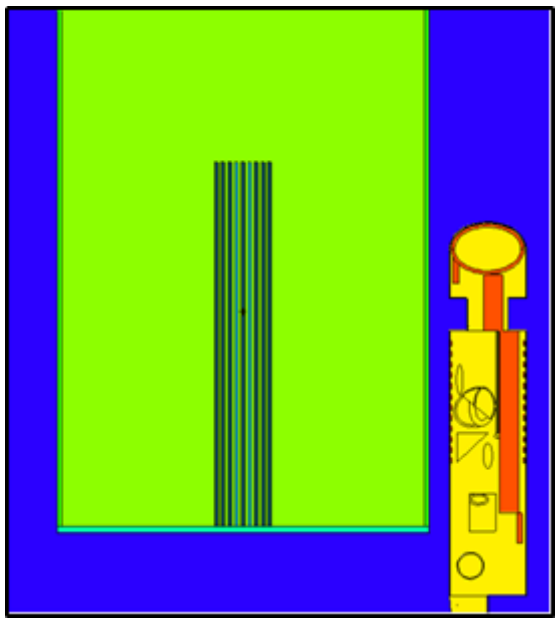

Figure A.4: Illustration of finished fuel assembly using MCNPX Visual Editor [13]. Assembly is pictured from the side.

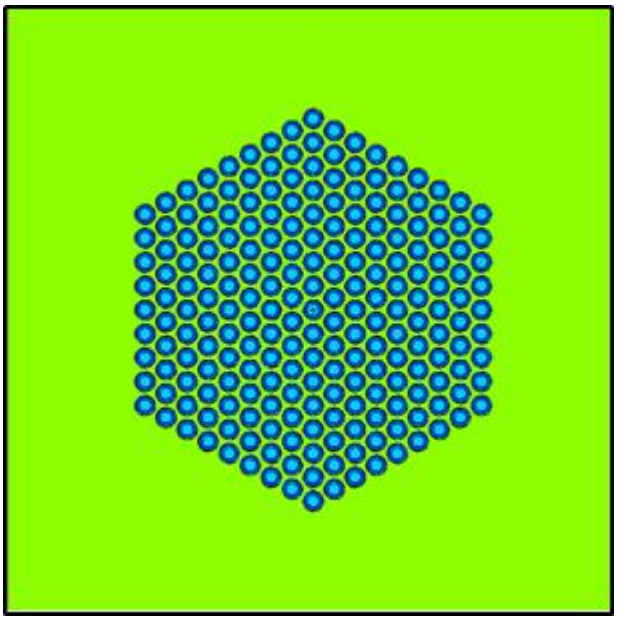

Figure A.5: Illustration of finished fuel assembly using MCNPX Visual Editor. Assembly is pictured from above.

Appendix B: Dose Rate Data

Task (Geometry)	Effective Dose Rate, $\dot{E}$ (mrem/h) UZr	UPuAmZr-0.03	UPuAmZr-0.6
Weigh Alloy (LC)	$2.72x10^{-2}$	$1.17x10^{0}$	$1.08x10^{1}$
Load/Unload Furnace (LC)	$2.72x10^{-2}$	$1.17x10^{0}$	$1.08x10^{1}$
Crush Heel (LC)	$6.08x10^{-2}$	$1.87x10^{0}$	$1.87x10^{1}$
Inspect Cast Pins (CPA)	$6.08x10^{-2}$	$1.87x10^{0}$	$1.87x10^{1}$
Demold Cast Pins (CPA)	$6.08x10^{-2}$	$1.87x10^{0}$	$1.87x10^{1}$
Measure Cast Pins (CPA)	$6.08x10^{-2}$	$1.87x10^{0}$	$1.87x10^{1}$
Cut Cast Pins (CPA)	$6.08x10^{-2}$	$1.87x10^{0}$	$1.87x10^{1}$
Inspect Cut Pins (CPA)	$6.08x10^{-2}$	$1.87x10^{0}$	$1.87x10^{1}$
Load/Unload Jackets (FPA)	$5.58x10^{-2}$	$1.54x10^{0}$	$1.32x10^{1}$
Weld Jackets (FPA)	$5.58x10^{-2}$	$1.54x10^{0}$	$1.32x10^{1}$
Un-weld Jackets (FPA)	$5.58x10^{-2}$	$1.54x10^{0}$	$1.32x10^{1}$
Bond & Inspect (FA)	$2.38x10^{-1}$	$6.85x10^{0}$	$5.54x10^{1}$
De-bond (FA)	$2.38x10^{-1}$	$6.85x10^{0}$	$5.54x10^{1}$
Final Inspection (FA)	$2.38x10^{-1}$	$6.85x10^{0}$	$5.54x10^{1}$

Table B.1: Dose rate inputs for processes requiring the handling of fuel materials in non-consolidated configurations (Scenarios 1-10).

Task (Geometry)	Effective Dose Rates, $\dot{E}$ (mrem/h) UZr	UPuAmZr-0.03
Weigh Alloy (LC)	$2.72x10^{-2}$	$1.17x10^{0}$
Load/Unload Furnace (LC)	$2.72x10^{-2}$	$1.17x10^{0}$
Crush Heel (LC-CPA)	$4.81x10^{-2}$	$1.23x10^{0}$
Inspect Cast Pins (LC-CPA)	$1.69x10^{-1}$	$5.30x10^{0}$
Demold Cast Pins (2 CPA)	$7.92x10^{-2}$	$2.31x10^{0}$
Measure Cast Pins (2 CPA)	$7.92x10^{-2}$	$2.31x10^{0}$
Cut Cast Pins (2 CPA)	$7.92x10^{-2}$	$2.31x10^{0}$
Inspect Cut Pins (CPA-FPA)	$1.69x10^{-1}$	$4.89x10^{0}$
Load/Unload Jackets (CPA-FPA)	$2.43x10^{-1}$	$6.99x10^{0}$
Weld Jackets (2 FA)	$3.05x10^{-1}$	$8.97x10^{0}$
Un-weld Jackets (2FA)	$3.05x10^{-1}$	$8.97x10^{0}$
Bond & Inspect (3FA)	$4.41x10^{-1}$	$1.33x10^{1}$
De-bond (3FA)	$3.90x10^{-1}$	$1.17x10^{1}$
Final Inspection (3FA)	$3.90x10^{-1}$	$1.17x10^{1}$

Table B.2: Dose rate inputs for processes requiring the handling of fuel materials in consolidated glove box configurations (Scenarios 11 & 12).

Appendix C: Assumed Cost and Footprint Data

Unit	Price	Footprint
Casing Glove Box	$8,800,000.00	59.38 ft^2
Fuel-Handling Glove Box	$5,650,000.00	59.38 ft^2
Prepping Glove Box	$5,650,000.00	59.38 ft^2
Casting Chamber	$2,000,000.00	-
Vacuum Pump	-	9.66 ft^2
Mold Removal Apparatus	$100,000.00	-
Inspection Station	$200,000.00	-
Pin Cutting Station	$100,000.00	-
Welding Station	$500,000.00	-
Pin Prep. Area	$100,000.00	-
He Leak Checker	$100,000.00	-

Table C.1: Representative pin production-related infrastructure costs [14].

Unit	Price	Footprint
Na-Bonding Lane	$100,000.00	-
Na-Extrusion Device	$100,000.00	-
Jacket Cutting Station	$1,370.00	20.25 ft^2
Jacket Bending Station	$5,100.00	20.25 ft^2
Jacket Welding Station	$10,000.00	20.25 ft^2
Jacket Inspection Station	-	20.25 ft^2
Crucible Coating Station	$6,686.00	19.41 ft^2
Crucible Oven	$2,160.00	19.41 ft^2
Vycor Coating Station	$6,686.00	19.41 ft^2
Vycor Oven	$2,160.00	19.41 ft^2
Vycor Inspection Station	-	19.41 ft^2

Table C.2: Representative non-pin production-related infrastructure costs.

Material	Cost
Fuel Alloy	$20,000.00 / kg
Metallic Sodium	$3.04 / kg
Vycor Mold	$30.70 / unit
Y_2O_3	$1,580.00 / kg
Graphite Crucible	$290.00 / unit
Type 304 SS	$236.00 / m^2
Sub-Assembly Ends	$1,000.00 / unit
Sub-Assembly Grids	$1,000.00 / unit

Table C.3: Representative material costs [15].

Employee Type	Wages
General Labor	$22 / hr
Welders	$22 / hr

Table C.4: Assumed employee wages [16].

References

[1] Hermann, O. W., Renier, J. P., & Parks, C. V. (1994). *Technical Support for a Proposed Decay Heat Guide Using SAS2H/ORIGEN-S Data. NUREG/CR-5625* (Report ORNL-6698). Oak Ridge, TN: Oak Ridge National Laboratory.

[2] Werner, C. J. (2018). *MCNP6.2 Release Notes* (Report LA-UR-18-20808). Los Alamos, NM: Los Alamos National Laboratory.

[3] Imagine That Inc. (2018). ExtendSim Pro 10 [Computer software]. San Jose, California.

[4] Crawford, D. C (2018). Versatile Test Reactor Startup Fuel Update [PowerPoint slides].

[5] Rao, N., Hagemeyer, D. A., & Holcomb, D. B. (2017). *Occupational Radiation Exposure Report for Calendar Year 2018*. Retrieved from https://energy.gov/ehss/occupational-radiation-exposure

[6] Pasamehmetoglu, K. (2019). Versatile Test Reactor Overview [Conference presentation]. Advanced Reactor Summit VI, San Diego, California, United States.

[7] Goorley, T. (2008). *MCNP Medical Physics Geometry Database. Los Alamos National Laboratory* (Report LA-UR-08-2468).

[8] Idaho National Laboratory (INL) (n.d.). *Special Nuclear Materials Glovebox*. Retrieved from https://mfc.inl.gov/SitePages/Instruments/Fuel%20Manufacturing%20Facility/Special%20nuclear%20materials%20glovebox.aspx

[9] International Commission on Radiological Protection (ICRP) (2012). Compendium of Dose Coefficients Based on ICRP Publication 60. ICRP Publication 119. Ann. ICRP 41(suppl.).

[10] Walter, C. M., Golden, G. K., & Olson, N. J. (1975). *U-Zr-Pu Metal Alloy: A Potential Fuel for LMFBR's* (Report ANL-76-28). Argonne, IL: Argonne National Laboratory.

[11] Bourque, C. M. (2021). Production through simulation: using simulation technologies to create and evaluate nuclear fuel fabrication facility designs [Master's thesis, The University of Texas at Austin]. Texas ScholarWorks

[12] Hezir, J. S. (2015). Perspectives on National Laboratory Cost Accounting Issues: Commission to review the effectiveness of the national energy laboratories.

[13] Schwarz Software & Consulting, LLC (2011). MCNPX Visual Editor (*Ver. 2.7.E.*) [Computer software].

[14] Kornreich, D. (2020). Representative glove box prices [personal communication].

[15] International Atomic Energy Agency (IAEA). (2010). *Cost aspects of the research reactor fuel cycle* (No. NG-T-4.3). Vienna, Austria.

[16] Parga, J. R., Jr. (2017). Constrained black box optimization for radioisotope thermal generator manufacturing [Master's thesis, The University of Texas at Austin]. Texas ScholarWorks.